

Some Surfactant Effect on the Electropolishing of Copper in H_3PO_4 Acid Compulsory Convection Circumstances: Agitated Vessel

Fatma M. Abouzeid ^{a*} Sultanah Alshammery ^b

^a Basic Science Department, Deanship of Preparatory Year, Imam Abdulrahman bin Faisal University, King Faisal Road, King Faisal City, Dammam, 34212, Saudi Arabia

^b Department of Basic Engineering Science, College of Engineering, Imam Abdulrahman bin Faisal University, King Faisal Road, King Faisal City, Dammam, 34212, Saudi Arabia

*E-mail: fmabouzeid@iau.edu.sa

Abstract

Copper electro-dissolution in phosphoric acid is investigated in different surfactant concentrations (Triton -x100, SAS, and CPC). The results reveal that surfactants have strong retardation behavior. Copper dissolution behavior in SAS-containing solution was examined beneath an agitated vessel using an impeller as compulsory convection. The limiting current increases with increasing rotation, which indicates that the anodic dissolution is a diffusion-controlled process. The limiting current was reduced by raising the SAS concentration and amplifying the temperature from 293 -313 K. The activation energy values established the reaction rate, which was controlled via diffusion. The data in different instances was commanded through dimensionless correlations of Sherwood (Sh), Schmidt (Sc), and Reynolds (Re) numbers.

Keywords: Copper, surfactant, Flory Huggins model, Kinetic thermodynamic model, Dimensionless correlations

Introduction

Copper alloys include bronze, brass, and copper-tin-zinc, which was strong enough to make guns and cannons and was known as a gun. Copper is perfectly designed for electric wiring because it is handled, can be drained into good cable, and has elevated electrical conductivity [1].

Metallic anodes are broadly used in electrochemical engineering.

1- An anode must dissolve with immediate smoothing and brightening of the surface (electropolishing). Electropolishing is surface finishing that occurs via a chemical

Received: 02 January 2025

Revised: 09 January 2025

Accepted: 17 January 2025

Copyright ♥ authors 2025

313

DOI: <https://doi.org/10.5281/ZENODO.14680390>

technique via which metal surface ion by ions is removed electrically. The main purpose is to diminish the metal microroughness. Therefore, noticeably dipping the product dust remains or sticking, improving the surface cleanability. Electropolishing is also used for deburring brightening and passivating[2]. The major electropolishing motive inserts are soft and silky surface production and make an inactive oxide coating to diminish the deterioration rate; electropolishing also eases outstanding pressure. Precise electrolyte formulations are fundamental for alloys and metals electro-polishing [3,4].

2-The anode dissolution must be selective, i.e. one of the components of the anode material is to dissolve quantitatively, while the others must not dissolve at all. An example is the electrolytic refining of copper. In this manner, copper dissolves as cupric ions, while noble metals stay intact and gather at the bottom in sludge form [5, 6].

It is well acknowledged that corrosion never stops but its capacity and seriousness may be diminished. Adding surfactants into aggressive media such as acid solutions is one of the methods for attaining this target. Surfactants are organic molecules with a chemical structure combining a polar (amphiphobic) and a nonpolar (amphiphilic) group into a single molecule. When dissolved in a solvent at low concentration, they can adsorb (or locate) at interfaces, thereby altering the interfaces' physical properties. Micellization is monitored in surfactant solutions when the concentration exceeds the critical micelle concentration (CMC), whereas the physicochemical properties of the aqueous solution modify immediately [3]. Surfactants are particles that may be found in an assembly of domains, from industrial settings to research laboratories, and are part of our daily lives. Owing to their distinctive structure, they may significantly alter the interfacial properties. This effect is important for industrial processes such as flotation, the cosmetic and food industries, drug delivery, emulsification, chemical mechanical polishing, as also for corrosion inhibition [4,5]. The studies on metal dissolution have been carried out under static conditions; therefore, the influence of flow on the dissolution process is an important issue to be considerable in the design and operation of industrial equipment. The most common type of flow conditions found in industrial processes is turbulent; however, few dissolution studies in controlled turbulent flow conditions are available. With the increasing necessity to describe the dissolution of metals in turbulent flow conditions, some laboratory hydrodynamic systems such as rotating cylinder electrodes (RCE) are used [6]. The use of a rotating cylinder and disc electrode in the dissolution process, fluid flow causes an increase in the rate of transport of chemical species to/from the metal surface, increasing the dissolution rate. Phosphoric acid (H_3PO_4) is widely used in the production of fertilizers and surface treatment of steel such as chemical and electrolytic polishing or etching, removal of oxide film, phosphating, passivating, and surface cleaning. The copper dissolution in phosphoric acid was studied previously in the presence of several additives [1-6]. Hence, this work aims to examine the dissolution behavior of copper anode in H_3PO_4 in an agitated vessel in the presence of surfactants (SAS) non -ionic surfactant namely Triton x-100, anionic surfactant namely sodium dodecyl sulfate (SDS), and cationic surfactants namely cetyl

pyridinium chloride (CPC). The adsorption of the surfactants on the metal surface can markedly change the dissolution–resisting property of the metal, so the study of the relationship between adsorption and dissolution inhibition is of great importance.

2. Materials and methods

The electrolyte solution was prepared from an analar grade of H_3PO_4 (85% w/w) supplied by BDH Chemicals Ltd. The selected non-ionic, anionic, and cationic surfactants were of clean excellence (>97%) and utilized without further purification. de-mineralized water was utilized in the solution preparation.

2.1. Solution preparation

8M H_3PO_4 and several surfactant concentration ranges of (5×10^{-7} to 1×10^{-2} M) have been prepared.

2.2. Electrochemical circuit

The cell consists of a rectangular container having the dimensions of 5×10 cm with electrodes fitting the whole cross-section. The electrodes were rectangular copper sheets 10 cm in height and 5 cm in width. Electrode separation was 5 cm. The electrical circuit consisted of a 6V D.C. Power supply, a variable resistance, and a multi-range ammeter connected in a series with a cell. A high-impedance voltmeter was connected in parallel with the cell to measure its potential. The steady-state anode potential was measured against a reference electrode consisting of copper wire immersed in a cup of lugging tube filled with phosphoric acid-surfactants solution like that in the cell. The tip of the lugging tube was placed 0.5–1mm from the anode wall. Polarization curves, from which the limiting current (I_L), was determined, were plotted by increasing the applied current stepwise and measuring the corresponding steady-state anode potential. Two minutes were allowed to reach the steady state potential. Before each run, the back of the anode was insulated with polystyrene lacquer, and the active surface was polished with fine emery paper, degreased with trichloroethylene, washed with alcohol, and finally rinsed in distilled water. The temperature was regulated by placing the cell in a thermostatic water bath at different temperatures (25, 30, 35, and 40°C). The copper used had the following chemical composition (Wt %): 0.0001 Cd, 0.001Ag , 0.003Ag , 0.003Pb , 0.005Sn and Cu is 99.98.

2.3. Scanning electron microscope

(JEOL, JSM-5300, scanning microscope, OXFORD instrument) has been used to investigate steel surfaces qualitatively

2.4. Agitated vessel

Agitation is a means of mixing phases and improving mass and heat transfer involving phases with peripheral surfaces.

A rotating impeller in a fluid imparts flow and clip to it, resulting from the flow of one portion of the fluid past another. Limiting cases of flow are in the axial or radial direction, so impellers are categorized appropriately in proportion to that of these streams is predominant.

Turbines with blades are inclined 45° C. Assemblies with four razor blades are used in the current work. Amalgamated axial and radial flow are accomplished remarkably successfully for heat exchange for heat exchange with vessel walls or internal coils.

When the greatest objective of these procedures is the performance of a chemical reaction, the accomplished specific rate is a suitable measure of the mixing quality. Comparisons in the achieved mass transfer coefficient are measures of their respective operations.

3. Result and discussion

3.1. Rotation effect

Fig .1. illustrates the dissolution polarization curve for the stationary copper electrode in 8 M H₃PO₄ in the absence and presence of SAS at several impeller rotations. The limiting current promotes progressively via raising the impeller speed, and this confirms the role played by diffusion in the reaction rate. Increasing impeller speed reduces the diffusion layer thickness across which Cu²⁺ diffuses from surface to bulk solution with a consequent improvement in the copper dissolution rate. Impeller rotation produces three fluid motion types in the agitated vessel, explicitly, axial flow, radial flow, and swirl flow [7,8].

Axial flow and radial flow are more efficient than swirl flow in improving the Cu²⁺ diffusion rate to the container border.

Axial flow increases the mixing settings and lowers stagnant pockets i.e. encourages the mass transfer rate via convection and decreases the flow diffusion contribution.

Impellers generally improve mass transfer performance, owing to the high-velocity gradient. The rotating operation should give higher turbulence strength and shear stress in the impeller zone than the co-rotating operation. Conversely, the mass transfer result acquired in this work for co-rotating and counter-rotating operations was efficiently the same. All these results indicate that improving the turbulence strength and shear stress in the impeller sweep-up region may not certainly produce a greater overall mass transfer performance [9].

Fig .2. shows the influence of impeller rotation speed on the limiting current density, the data fit the equation

$$i_L = a \omega^{0.36} \quad (1)$$

The exponent 0.36 is in fair agreement with the value obtained by authors who studied mass and heat transfer at the wall of an agitated vessel.

3.2.Effect of electrode height

Received: 02 January 2025

Revised: 09 January 2025

Accepted: 17 January 2025

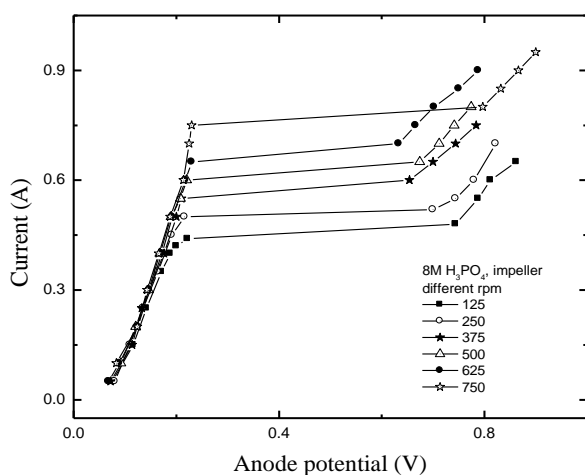
Copyright ♥ authors 2025

DOI: <https://doi.org/10.5281/ZENODO.14680390>

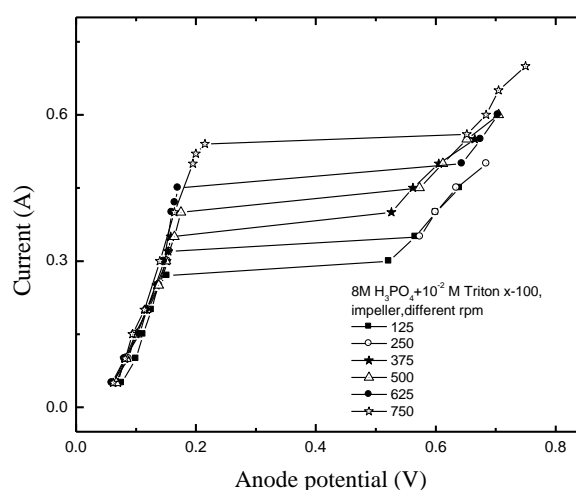
The reduction in the limiting current density with cumulative electrode height is credited to the growth in the hydrodynamic boundary layer breadth and diffusion layer thickness with growing electrode height consistent with the hydrodynamic boundary layer concept however the proponent -0.30 , is at variance with the theoretical value (-0.5) predicted from the hydrodynamic boundary theory for axial flow past a flat plate. This divergence may be ascribed to

- the presence of a downward-moving natural convection stream that arises from the difference in density among the interfacial solution that comprises saturated copper phosphate in H_3PO_4 and the solution bulk that contain only H_3PO_4 . the downward inspiring natural convection stream convinced via impeller[10]

Fig .3. Explain the effect of plate height on the limiting current density , the data fit the equation $i_L = 0.67 L^{-0.30}$ (2)



a
c



b
D

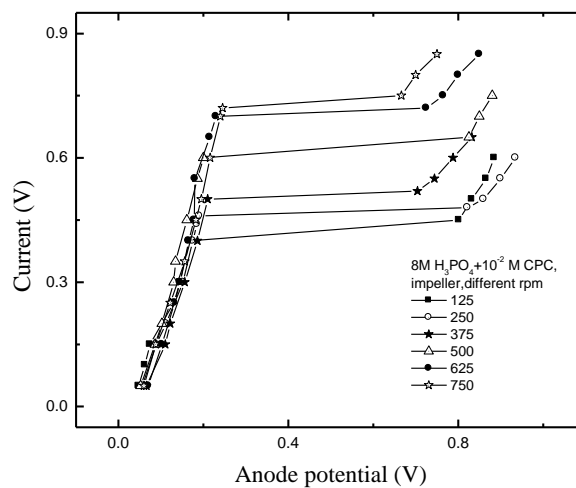
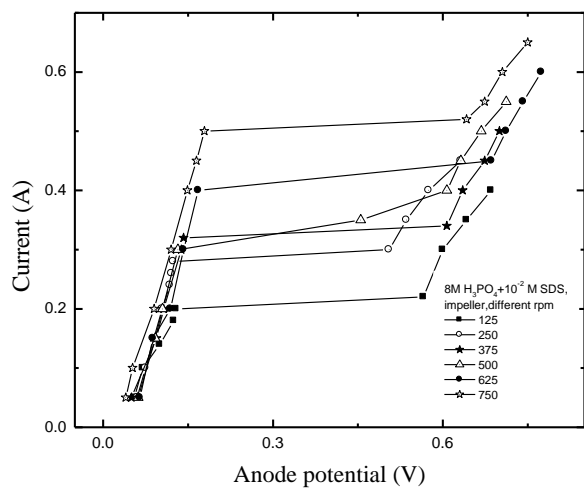
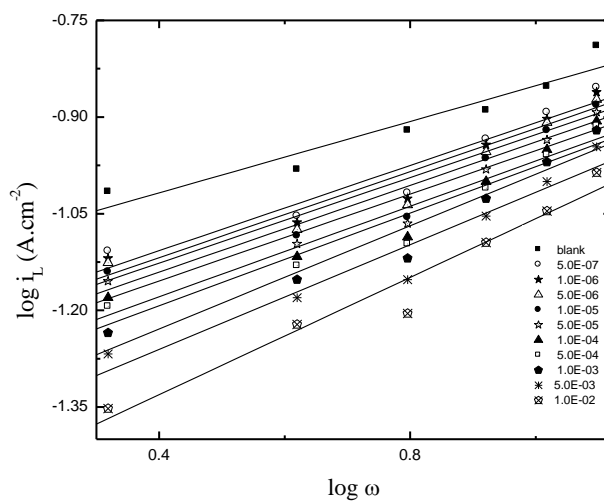
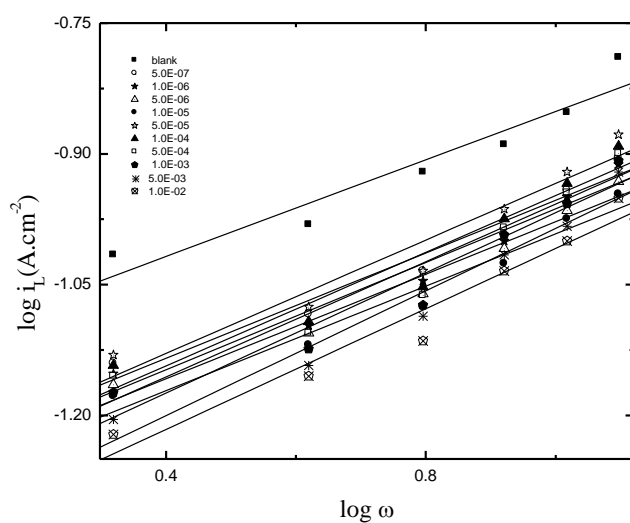
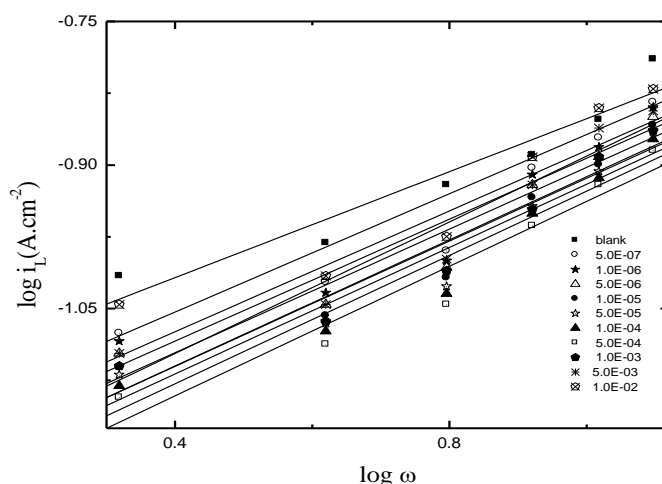


Fig .1. Anodic polarization curve for rotating copper stationary electrode at different impeller rotation . A)in 8 M H₃PO₄ free solution .b)in presence 10⁻² M Triton x-100 , c) 10⁻² M SDS and d) 10⁻² M CPC.



a

b



c

Fig.2.Effect of impeller rotation speed on limiting current ($\log i_L$ Vs. $\log \omega$)

- Rotation and interference with its effect on the hydrodynamic boundary layer thickness and diffusion layer thickness.
- It is also well known that in agitated vessels that use axial flow impellers such as the present case, axial flow is accompanied by radial and swirl flow, especially in the absence of baffles. Under such situations, radial flow and swirl flow intervene with the effect of axial flow on the hydrodynamic boundary layer thickness and diffusion layer thickness. i.e. the axial flow impellers exist to be equally effectual and extensively more efficient than the radial and swirl flow [11]

3.3. SAS concentration on the dissolution process

The copper dissolution rate in 8 M H_3PO_4 in the absence and presence of SAS in an agitated vessel applying a rotating impeller at 375 rpm is explained in Fig .4 and Table 2 , the limiting current decreases as the concentration of SAS increases i.e. dissolution inhibition enhances with the SAS concentration . This behavior is ascribed to the fact that the adsorption amount and converge of SAS on copper surface increase with the SAS concentration.

$$IE \% = \frac{I_{L(blank)} - I_{L(SAS)}}{I_{L(blank)}} \times 100 \quad (3)$$

Surfactants are distinctive molecules composed of a polar hydrophilic group (Head) attributed to a non-polar hydrophobic tail (Tail). The surfactants reduce the dissolution process due to the presence of numerous active clusters for adsorption along hydrocarbon chain that confirm large surface coverage. The surfactants polar group is accountable for the covalent type bond formation with the active sites of the metal surface. The surfactant's non-polar group forms a hydrophobic barrier and

successfully screens the metal from the aggressive attack of phosphate ion in the environment [12].

Table 2 , compare the retardation behavior of the three studied surfactants. it is found that retardation behavior is concentration and SAS-type dependent.

The limiting current reduces and IE % increases as Triton x-100 concentration up to 1×10^{-5} mol/l , at 5×10^{-5} , limiting current and consequently IE % reduces after that (1×10^{-4} - 1×10^{-2} mol/l) as concentration of Triton x-100 increases, the limiting current decrease and IE % increases. The inhibition behavior of Triton x-100 can be ascribed to the lengthy hydrocarbon chain forming a closed network structure, which prevents the approach of the aggressive ions to the metal surface.

When the micelle formed (at 5×10^{-5} mol/l) the large size of the micelle of Triton x-100 led to a porous network structure on a copper surface so IE % decreased. But when concentration exceeds the CMC value, higher retardation efficiency is obtained. In more detail, at low concentrations, the surfactant monomers were adsorbed as individual ions/molecules. At higher concentrations, tail-tail interactions of Triton x-100 may begin to cause association of the adsorbed SAS aggregates into an additional coverage beyond the monolayer i.e. micelle or bilayer formation.

The surfactant monomer head group of the first layer faces the surface while those of the second layer face the bulk solution. thus, increasing the surface coverage from coverage at low surfactant to bilayer coverage at higher SAS concentration. So IE % increases at higher concentrations [13].

Further inspection of Table 2 , it is observed that limiting current (dissolution rate) decreases and IE % increases as SDS concentration increases reaching a maximum value at 1×10^{-2} mol/l SDS. Anionic surfactant SDS inhibits the dissolution process by getting adsorbed electrostatically on the positively charged copper surface

It is well known that IE increases with increasing SAS concentration until it reaches a maximum value. This value corresponds to the CMC and the inhibition efficiency of metal slightly changes when the SAS concentration exceeds the critical micelle concentration

In SDS case, the high inhibition efficiency is obtained at a concentration above CMC . We can suggest that due to micelle formation. The micelle is highly charged, and because of higher electrostatic attraction, adsorption of SDS on the copper surface increases and IE % increases.

In spite of CPC behavior, it is found that limiting current decreases and IE % increases as CPC concentration increases up to CMC formation (1×10^{-3}) when the concentration exceeds CMC the acceleration in dissolution rate is observed [14].

The retardation influence of CPC in the H_3PO_4 solution may be clarified as follows
CPC may be classified as 1:1 electrolyte, it may be ionized in the acid solution as following $CPC \rightarrow CP^+ + Cl^-$

Thus in an aqueous acidic solution, CPC exists in the cation organic part CP^+ and the anion inorganic part Cl^- . It is well known that the copper surface charges positively in

an acidic solution, so it is difficult for CP^+ to approach the positively charged copper surface due to electrostatic repulsion. the Cl^- ions could accumulate gradually closely to the copper/ solution interface being specifically adsorbed, they create an excess negative charge toward the solution and favor more adsorption of the cations, the CP^+ may adsorb through electrostatic interaction between the positively charged molecules and negatively charged metal surface. In other words, there may be synergism between CP^+ and Cl^- [15].

The acceleration in copper dissolution observed beyond CMC (1×10^{-3} mol/l) may be attributed to when CPC micelle formed convey concentrated positively charged heads with concentrated negatively charged chloride counter ions , the higher concentration of aggressive chloride ions which initiate copper dissolution promotion

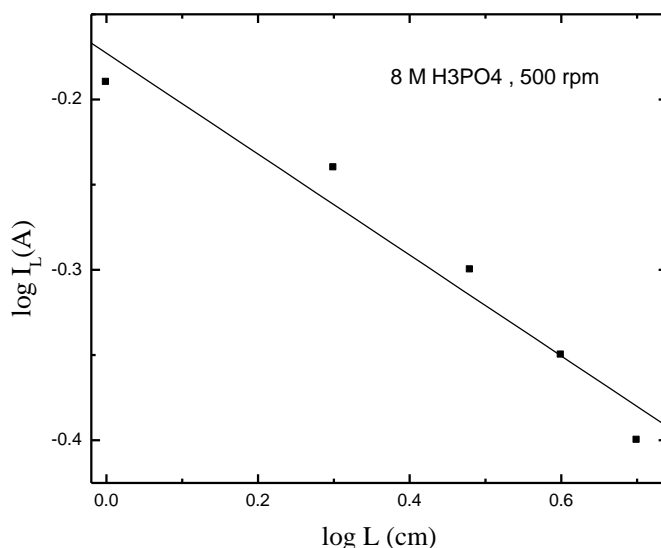


Fig. 3. Effect of anode height on the limiting current

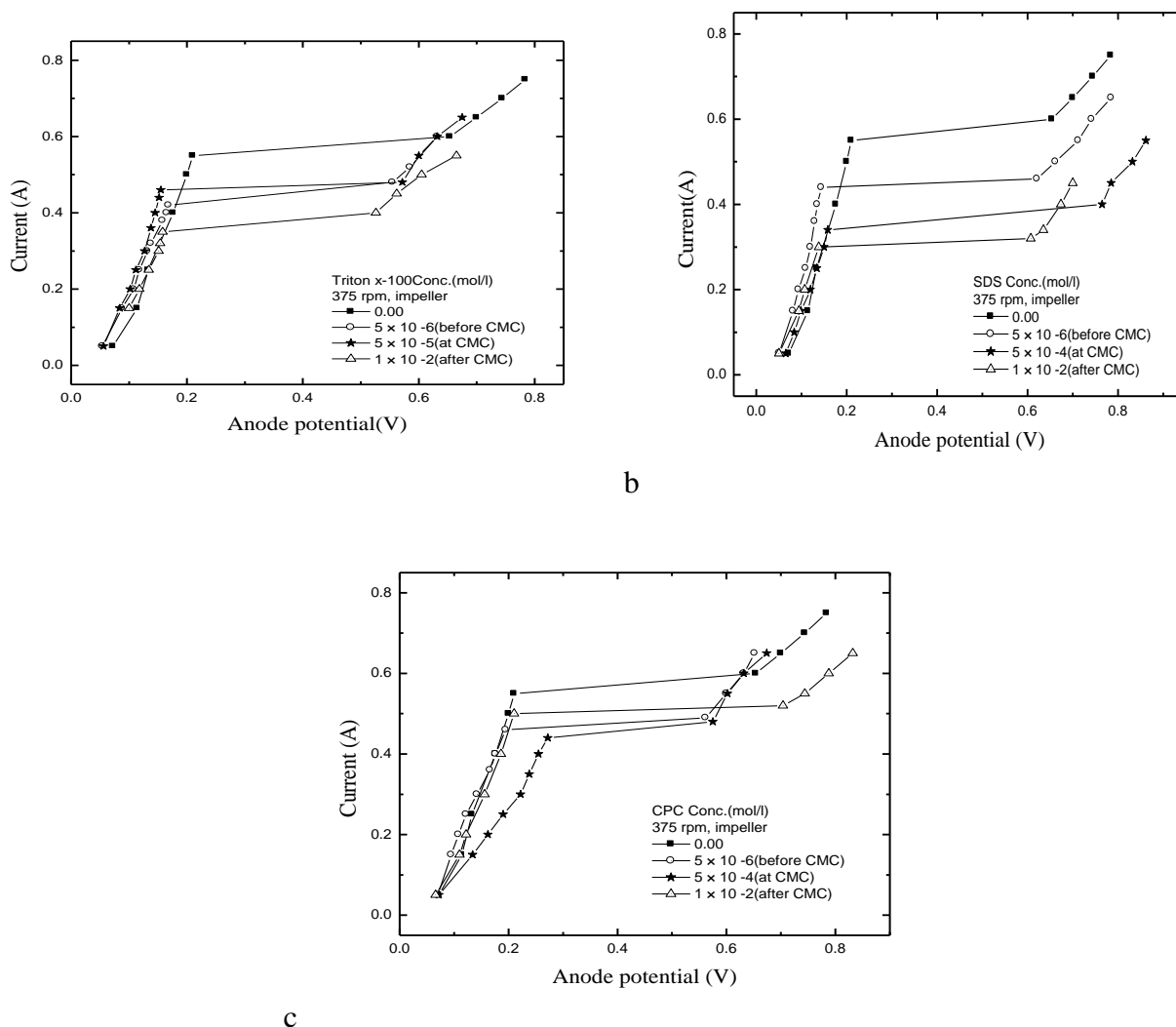


Fig .4. Anodic polarization curve for rotating copper stationary electrode at different impeller rotation . in the absence and presence of different concentrations of SAS , a) Triton x-100 b)SDS and c) CPC.

3.4. Temperature effect

The temperature may alter the interaction between the working electrode surface and the acidic medium. To gain more information about the adsorption type and the efficiency of the studied SAS at elevated temperatures, the dissolution process was performed at several temperatures (25-40 ° C) for copper in 8 M H₃PO₄ without and with the nominated concentration of the considered surfactant.

Fig .5. Show the polarization curve for the dissolution process in the absence and presence of SAS for copper metal at several temperature.

In the studied temperature, are remarkable variation in dissolution rate is found with growing temperature, as predictable the limiting current improves with improving temperature for 8 M H₃PO₄ and 8 M H₃PO₄ containing SAS solution . The SAS effect

shows to be solution temperature dependent. Some studies have illuminated this phenomena by the desorption of the SAS molecules from the copper metal at higher temperature leading to impressive area of copper metal being exposed to H_3PO_4 solution (aggressive solution) [16].

The data exhibits that the retardation efficiency reduces with improving temperature for all examined temperature (Table 2) . Fig .6. represent the relation between retardation efficiency and SAS concentration at several temperature. This behavior may be ascribed to reduce in the strength of adsorption process at elevated temperature, suggesting that physical adsorption may be the predominant mechanism of adsorption of SAS on copper surface [17].

Table .2. values of limiting current density $I_L(A)$ and % inhibition using impeller in 8M H_3PO_4 in absence and presence of SAS at 375 rpm and different temperature									
Conc.	SAS	25° C		30° C		35° C		40° C	
		$I_L(A)$	%IE	$I_L(A)$	%IE	$I_L(A)$	%IE	$I_L(A)$	%IE
0.0	Triton x-100	0.600	-	0.750	-	0.872	-	0.986	-
5.0E-07		0.462	23.00	0.582	22.71	0.700	19.72	0.812	17.65
1.0E-06		0.450	25.00	0.571	24.17	0.688	21.10	0.800	18.86
5.0E-06		0.435	27.50	0.550	26.96	0.672	22.94	0.780	20.89
1.0E-05		0.420	30.00	0.532	29.35	0.652	25.23	0.770	21.91
5.0E-05		0.462	23.00	0.588	21.91	0.712	18.35	0.810	17.85
1.0E-04		0.443	26.17	0.560	25.63	0.690	20.87	0.790	19.88
5.0E-04		0.433	27.83	0.546	27.49	0.675	22.59	0.774	21.50
1.0E-03		0.422	29.67	0.532	29.35	0.660	24.31	0.760	22.92
5.0E-03		0.410	31.67	0.520	30.94	0.648	25.69	0.745	24.44
1.0E-02		0.384	36.00	0.500	33.60	0.630	27.75	0.722	26.77
0.0	SDS	0.600	-	0.750	-	0.872	-	0.986	-
5.0E-07		0.480	20.00	0.620	17.66	0.730	16.28	0.850	13.79
1.0E-06		0.470	21.67	0.608	19.26	0.720	17.43	0.840	14.81
5.0E-06		0.460	23.33	0.594	21.12	0.710	18.58	0.825	16.33
1.0E-05		0.440	26.67	0.570	24.30	0.692	20.64	0.812	17.65
5.0E-05		0.430	28.33	0.560	25.63	0.674	22.71	0.782	20.69
1.0E-04		0.410	31.67	0.540	28.29	0.654	25.00	0.762	22.72
5.0E-04		0.400	33.33	0.524	30.41	0.634	27.29	0.744	24.54
1.0E-03		0.380	36.67	0.500	33.60	0.622	28.67	0.724	26.57
5.0E-03		0.352	41.33	0.466	38.11	0.590	32.34	0.700	29.01
1.0E-02		0.312	48.00	0.422	43.96	0.550	36.93	0.650	34.08
0.0	CPC	0.600	-	0.750	-	0.872	-	0.986	-
5.0E-07		0.512	14.66	0.650	13.68	0.762	12.61	0.895	9.23
1.0E-06		0.500	16.66	0.640	15.01	0.752	13.76	0.875	11.26
5.0E-06		0.492	18.00	0.625	17.00	0.741	15.02	0.860	12.78
1.0E-05		0.480	20.00	0.615	18.33	0.725	16.86	0.845	14.30
5.0E-05		0.470	21.67	0.605	19.65	0.715	18.00	0.832	15.62
1.0E-04		0.462	23.00	0.590	21.65	0.700	19.72	0.812	17.65
5.0E-04		0.450	25.00	0.570	24.30	0.690	20.87	0.800	18.86
1.0E-03		0.488	18.67	0.614	18.45	0.730	16.28	0.832	15.62
5.0E-03		0.502	16.33	0.633	15.93	0.753	13.65	0.855	13.29
1.0E-02		0.530	11.66	0.676	10.22	0.787	9.75	0.899	8.82

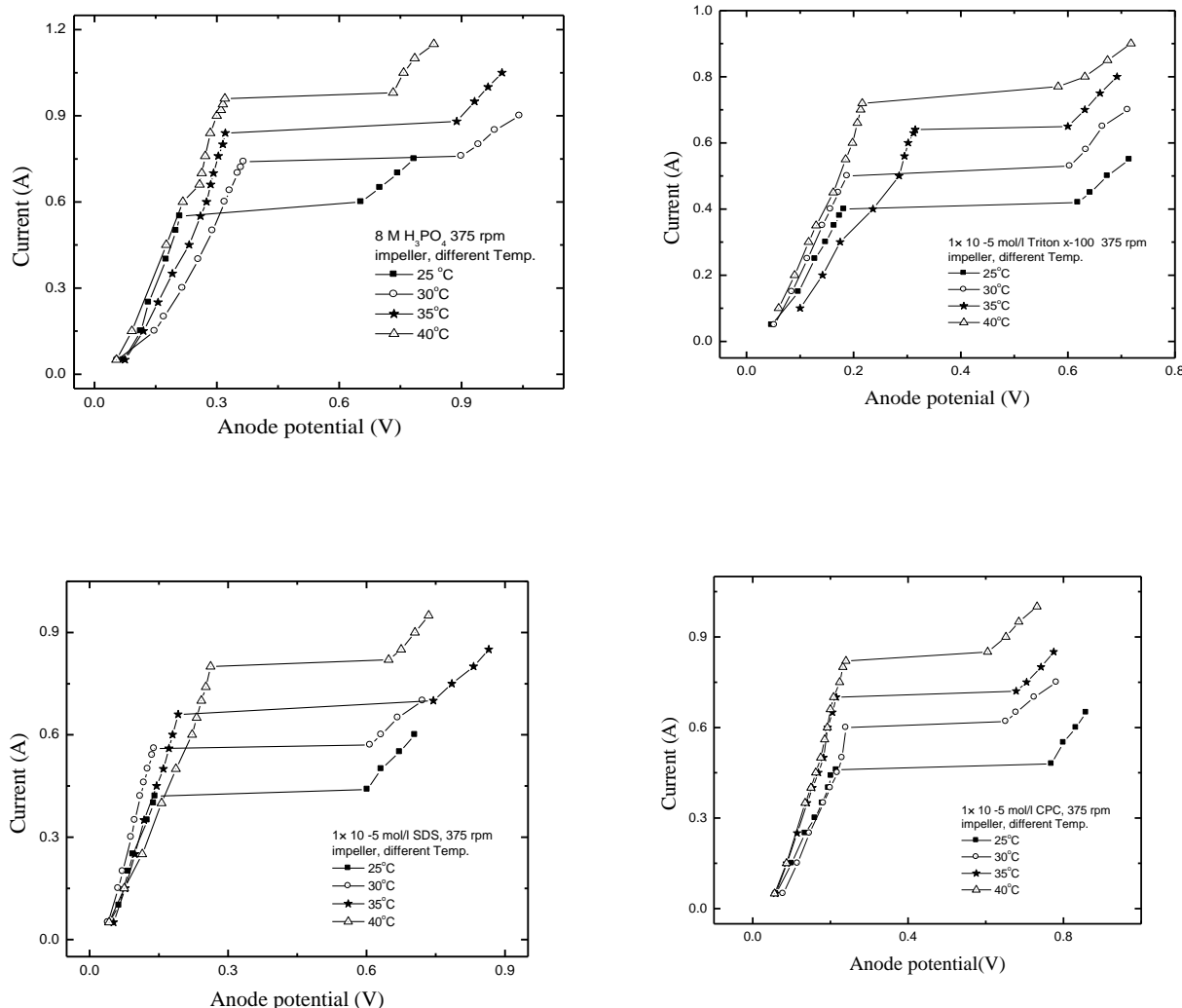
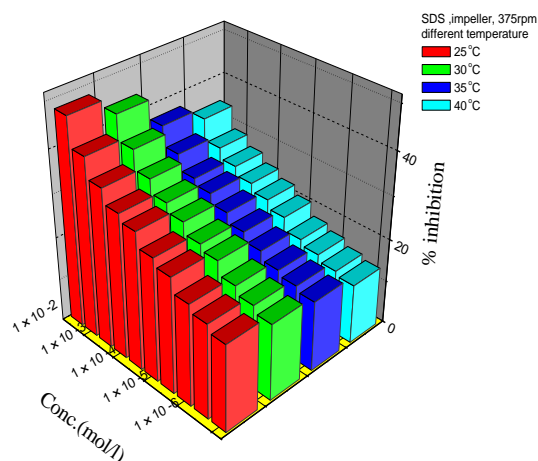
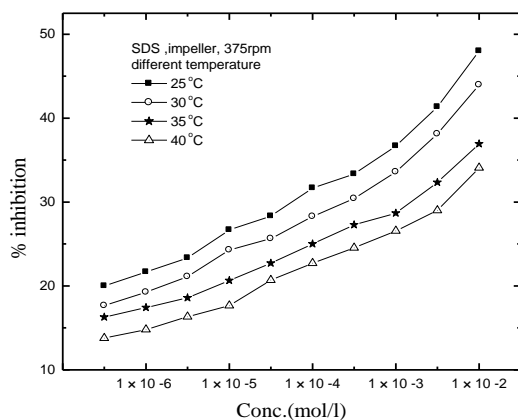
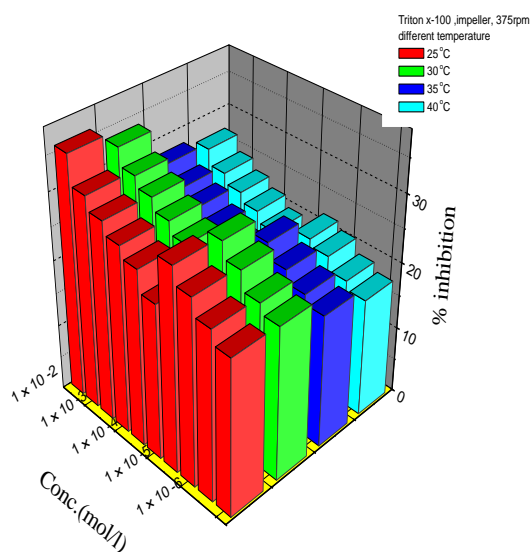
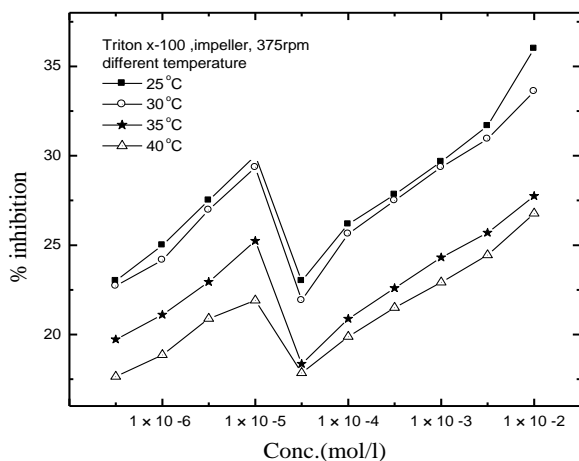


Fig .5. Anodic polarization curve for rotating copper stationary electrode at different temperature rotation . A)in 8 M H_3PO_4 free solution .b)in presence 10^{-5} M Triton x-100 , c) 10^{-5} M SDS and d) 10^{-5} M CPC.

a



b

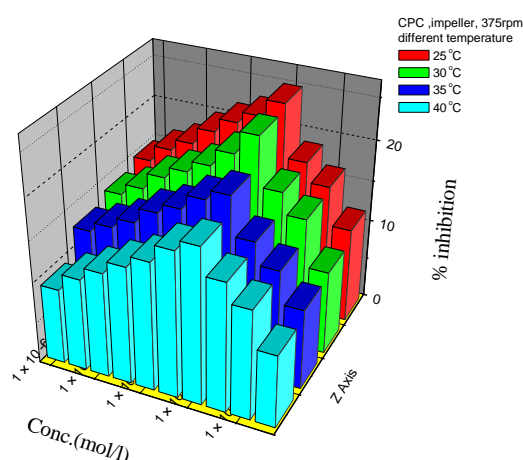
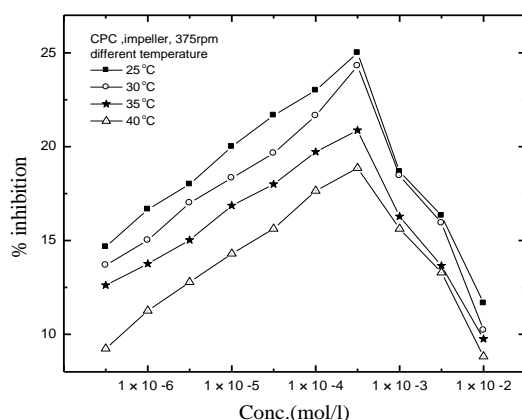


Fig .6. Variation of the inhibition efficiency with SAS concentration in 8M H_3PO_4 . a) Triton x-100, b) SDS and c) CPC at different temperatures.

3.5. Activated parameters

Arrhenius plot for the copper dissolution process in 8M H_3PO_4 in absence and presence of SAS in an agitated vessel using impeller rotate at 375 rpm in Fig .7

The activation energies may be estimated from the following set of equations

$$I_L = k \exp -E_a/RT \quad (4)$$

$$I'_L = k \exp -E'_a/RT \quad (5)$$

Where E_a , E'_a are the activation dissolution energies in the absence and presence of SAS respectively. T is the absolute temperature, k is the Arrhenius pre-exponential constant and R is the universal gas constant. Also, the activated parameters like free energy of activation $\Delta G^\#$, enthalpy of activation $\Delta H^\#$ and entropy of activation $\Delta S^\#$, were intended using the following equation

$$I_L = RT/Nh \exp \Delta S^\# /RT \exp - \Delta H^\# /RT \quad (6)$$

$$\Delta G^\# = \Delta H^\# - T \Delta S^\# \quad (7)$$

By plotting $\ln I_L/T$ against $1/T$ (Fig .8), $\Delta H^\#$ can calculated from the slope while $\Delta S^\#$ can calculated from the intercept of the plot. The obtained values of activated parameters are represented in Table 3

Inspection of Table 3, the result clearly shows that the SAS-containing solution has a higher value of E_a than the SAS-free solution (blank). This enhancement of E_a in the presence of SAS indicates more energy barriers for the dissolution process in the presence of SAS is attained.

The rise in activation energy value, when compared to the blank solution, is normally explained as an indication for the formation of adsorptive film. This fact is governed

Received: 02 January 2025

Revised: 09 January 2025

Accepted: 17 January 2025

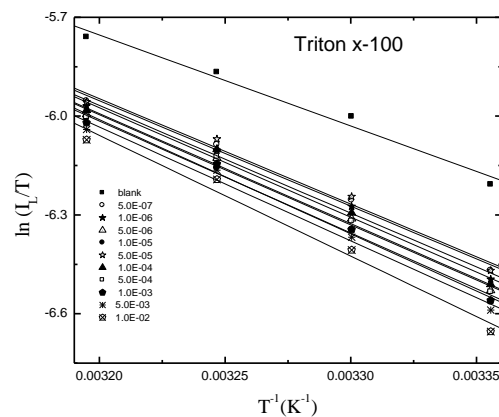
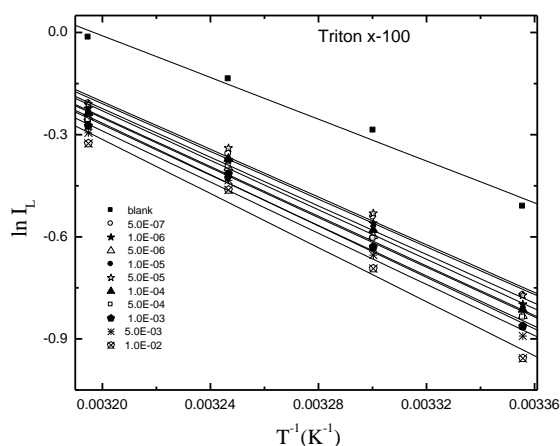
Copyright © authors 2025

DOI: <https://doi.org/10.5281/ZENODO.14680390>

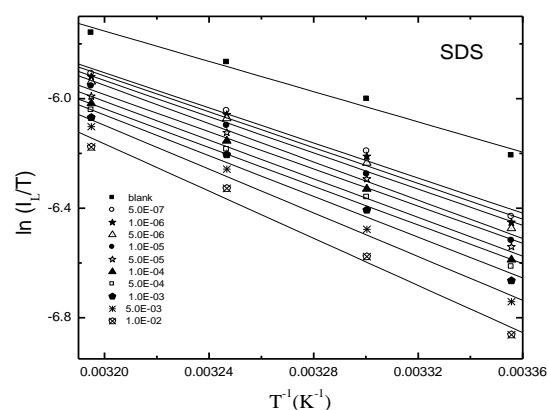
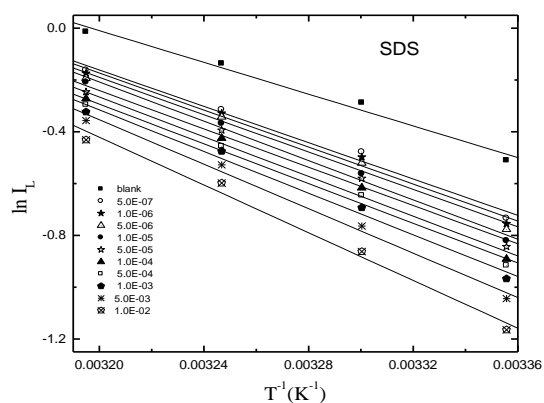
by a physical (electrostatic) mechanism between SAS molecules and the copper surface [18].

Further going over Table 3 it is found that $\Delta G^\#$ for the solution containing SAS is greater than SAS free solution (blank) revealing that in cores of SAS addition , the activated complex for the dissolution process is less stable as compared to its absence . The positive sign of $\Delta H^\#$ showed the endothermic nature of copper dissolution process . The values of $\Delta S^\#$ were lower for inhibited solution than that for the uninhibited solution. This suggests that decrease in randomness occurred on going from reactant to the activated complex in presence of SAS [19].

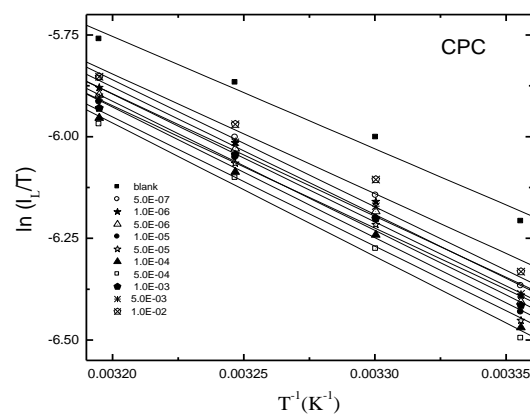
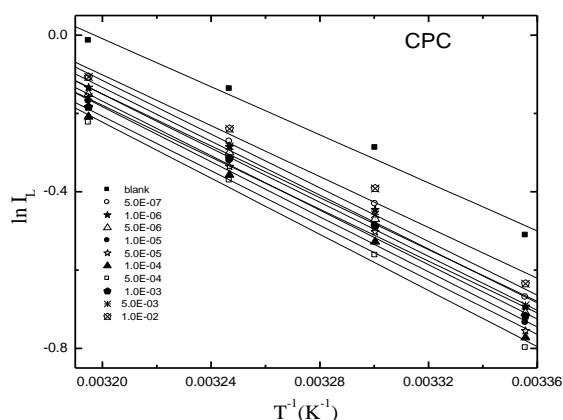
Table. 3. electropolishing activated parameters for copper stationary electrode in agitated vessel using impeller rotate at 375 rpm in absence and presence of SAS					
Conc. Mol.l ⁻¹	SAS	E _a (kJ/mol)	$\Delta H^\#$ (kJ/mol)	$-\Delta S^\#$ (J/mol.K)	$\Delta G^\#$ kJ/mol)
Blank	0.0	25.47±2.378	22.99 ±2.378	171.83 ± 7.78	74.22 ± 4.699
5.0E-07	Triton x-100	29.18 ± 1.726	26.70 ± 1.726	161.63 ± 5.65	74.89 ± 3.411
1.0E-06		29.70 ± 1.844	27.26 ± 1.844	159.95 ± 6.04	74.95 ± 3.644
5.0E-06		30.35 ± 1.796	27.88 ± 1.796	158.19 ± 5.879	75.04 ± 3.549
1.0E-05		31.43 ± 1.395	28.95 ± 1.395	154.91 ± 4.56	75.13 ± 2.757
5.0E-05		29.18 ± 2.457	26.70 ± 2.457	161.56 ± 8.04	74.87 ± 4.855
1.0E-04		30.24 ± 2.183	27.76 ± 2.183	158.42 ± 7.14	74.99 ± 4.314
5.0E-04		30.40 ± 2.110	27.91 ± 2.110	158.08 ± 6.90	75.05 ± 4.170
1.0E-03		30.80 ± 2.011	28.32 ± 2.011	156.96 ± 6.58	75.12 ± 3.974
5.0E-03		31.28 ± 2.200	28.81 ± 2.200	155.55 ± 7.19	75.18 ± 4.346
1.0E-02	SDS	33.06 ± 2.874	30.58 ± 2.874	150.08 ± 9.41	75.33 ± 5.680
5.0E-07		29.21 ± 2.415	26.73 ± 2.415	161.14 ± 7.90	74.77 ± 4.772
1.0E-06		29.72 ± 2.368	27.24 ± 2.368	159.58 ± 7.75	74.83 ± 4.680
5.0E-06		30.03 ± 2.342	27.55 ± 2.342	158.73 ± 7.66	74.88 ± 4.63
1.0E-05		31.60 ± 2.129	29.12 ± 2.129	153.86 ± 6.96	75.00 ± 4.20
5.0E-05		30.79 ± 2.559	28.31 ± 2.559	156.72 ± 8.38	75.04 ± 5.06
1.0E-04		31.90 ± 2.724	29.42 ± 2.724	153.37 ± 8.91	75.15 ± 5.38
5.0E-04		31.92 ± 2.430	29.44 ± 2.430	153.55 ± 7.95	75.22 ± 4.80
1.0E-03		33.48 ± 2.67	31.00 ± 2.67	148.76 ± 8.72	75.35 ± 5.27
5.0E-03	CPC	35.74 ± 2.332	33.26 ± 2.332	141.84 ± 7.63	75.55 ± 4.61
1.0E-02		38.37 ± 2.99	35.89 ± 2.99	134.00 ± 9.79	75.84 ± 5.91
5.0E-07		28.52 ± 1.844	26.14 ± 1.844	162.95 ± 6.03	74.63 ± 3.64
1.0E-06		28.62 ± 2.207	26.14 ± 2.207	162.79 ± 7.22	74.67 ± 4.36
5.0E-06		28.70 ± 1.990	26.22 ± 1.990	162.67 ± 6.51	74.72 ± 3.93
1.0E-05		28.95 ± 2.172	26.47 ± 2.172	162.03 ± 7.11	74.78 ± 4.29
5.0E-05		29.25 ± 2.306	26.77 ± 2.306	161.19 ± 7.55	75.00 ± 4.56
1.0E-04		28.97 ± 2.134	26.49 ± 2.134	162.27 ± 6.98	74.87 ± 4.22
5.0E-04		29.81 ± 1.863	27.33 ± 1.863	159.71 ± 6.10	74.95 ± 3.68
1.0E-03		27.58 ± 2.148	25.11 ± 2.148	166.47 ± 7.03	74.74 ± 4.24
5.0E-03		27.55 ± 2.292	25.07 ± 2.292	166.34 ± 7.50	74.67 ± 4.53
1.0E-02		27.03 ± 2.553	24.55 ± 2.553	167.61 ± 8.35	74.52 ± 5.04



a



b



c

Fig .7. Arrhenius plot of the electropolishing process recorded for stationary copper electrode in agitated vessel using impeller rotate at 375rpm in 8M H_3PO_4 solution containing different

Fig .8. Transition state plot of the electropolishing process stationary copper electrode in agitated vessel using impeller rotate at 375rpm in 8M H_3PO_4 solution containing

Received: 02 January 2025

Revised: 09 January 2025

Accepted: 17 January 2025

Copyright © authors 2025

DOI: <https://doi.org/10.5281/ZENODO.14680390>

concentration of SAS (a); Triton x-100, (b,)SDS and (c)CPC different concentration of SAS (a); Triton x-100, (b,)SDS and (c)CPC

3.6. Adsorption isotherm

The sort and interaction scale among SAS and metallic surfaces have been extensively studied with the application of adsorption isotherm. The organic molecules adsorption occur owing to the interaction energy among SAS and metallic surface is greater than that among water molecules and metallic surface.

To attain the adsorption isotherm, the degree of surface coverage (θ) was established as function of SAS concentration. The values of (θ) were then plotted to fit the most suitable mode of adsorption.

$$\theta = \frac{I_L(\text{blank}) - I_L(\text{SAS})}{I_L(\text{blank})}, \quad (8)$$

Fig. 9 shows the dependency of the relationship C/θ as a function of SAS concentration (Triton x-100, SDS, and CPC) along with Langmuir isotherm. Plots yield a good fitting with a correlation factor of 0.99 but the slope of the isotherm deviates from unity. This deviation may be explained based on an interaction between the adsorbed SAS molecules on the copper surface by mutual repulsion or attraction

$$C/\theta = 1/K + C \quad (9)$$

The equation of Flory–Huggins isotherm is given by:

$$\log \theta / C = \log xK + x \log (1-\theta) \quad (10)$$

where x is the number of active sites concerned by one inhibitor molecule or number of water molecules substituted by one molecule of the adsorbate.

A plot of $\log \theta / C$ vs. $\log (1-\theta)$ (Fig.10), produces a straight line of a slope x and intercept $\log xK$ as shown in Fig. 10, which is valid for the used SAS. The data indicates that the values of X were approximately 30, 22, and 50 for Triton x-100, SDS and CPC respectively. The values of $x > 1$ implied that one inhibitor molecule replaces more than one water molecule [20].

Frumkin adsorption isotherm was found to fit well with the experimental data. The adsorption isotherm relationship of Frumkin is represented by the following equation

$$\ln \left[\frac{\theta}{C(1-\theta)} \right] = \ln K + 2a\theta \quad (11)$$

Fitting curves of the polarization data to Frumkin adsorption of copper in 8 M H_3PO_4 solution various SAS concentrations are shown in Fig. 11

Table .4 shows the values of K and a , where a is the lateral interaction term illustrating the molecular contact in the adsorption layer and the heterogeneity of the surface (it is measured for the steepness of the adsorption isotherm). It is found that

the negative value of a indicates that repulsion among molecules improves the adsorption energy with the improvement of θ [21].

The kinetic–thermodynamic model is given by:

$$\log \theta / (1-\theta) = \log K' + y \log C \quad (12)$$

where y is the number of inhibitor molecules occupying one active site. The binding constant K is given by:

$$K = K'^{(1/y)} \quad (13)$$

The slope y of the linear relation between $\log [\theta/(1-\theta)]$ versus $\log C$ (Fig.12) is less than unity, which means that the given additive molecule occupied more than one active site. Values of y and the number of active sites ($1/y$) of the metal surface that were occupied by one molecule of the organic additive under the present conditions are given in Table 4. It is concluded from the last values that the number of additive molecules that occupy one active site is less than unity in all cases. Also, the efficiency of the dissolution process is essentially the function of the magnitude of its binding constant K , large values of K mean better and, strong interaction which recorded for Triton x-100, whereas small values of K mean that the interaction between the additive molecules and metal surface is weaker which recorded for CPC [22].

The standard adsorption free energy ΔG° was obtained according to

$$\log K = -1.74 - (-\Delta G_{\text{ads}} / 2.303RT) \quad (14)$$

The ΔG° negative values (Table 5) suggest the SAS adsorption on copper surface is a spontaneous process and its low values are consistent with the electrostatic interaction between the charged molecules and the charged metals (physical adsorption) [23].

Table 4 : linear fitting parameters of SAS for agitated vessel using impeller rotate at 375 rpm and 25 ° C

Surfactant	Langmiur		Frumkin		Florry-Huggins		Kinetic adsorption isotherm		
	slope	K	A	K	x	K	y	1/y	K
Triton x-100 (before CMC)	2.8	4.5×10^3	-20.00	6.03×10^9	30.33	4.24×10^7	0.11	9.09	43.27
Triton x-100 (after CMC)	2.8	4.5×10^3	-20.00	6.56×10^7	29.05	3.14×10^5	0.10	9.82	0.200
SDS	2.12	4.4×10^3	-16.38	1.64×10^8	22.16	8.83×10^5	0.12	8.40	14.64
CPC	8.21	-800.00	-30.75	3.76×10^9	50.30	2.13×10^7	0.09	10.81	0.018

Table.5.calculated values of free energy of adsorption- $\Delta G_{ads}(kJ\ mol^{-1})$ for different surfactants at 25 °C for RDE at 375 rpm				
Surfactant	Triton x-100 (Before CMC)	Triton x-100 (after CMC)	SDS	CPC
$-\Delta G_{ads}^{\circ}$ (KJ/mol)				
	19.28	5.96	16.60	0.079

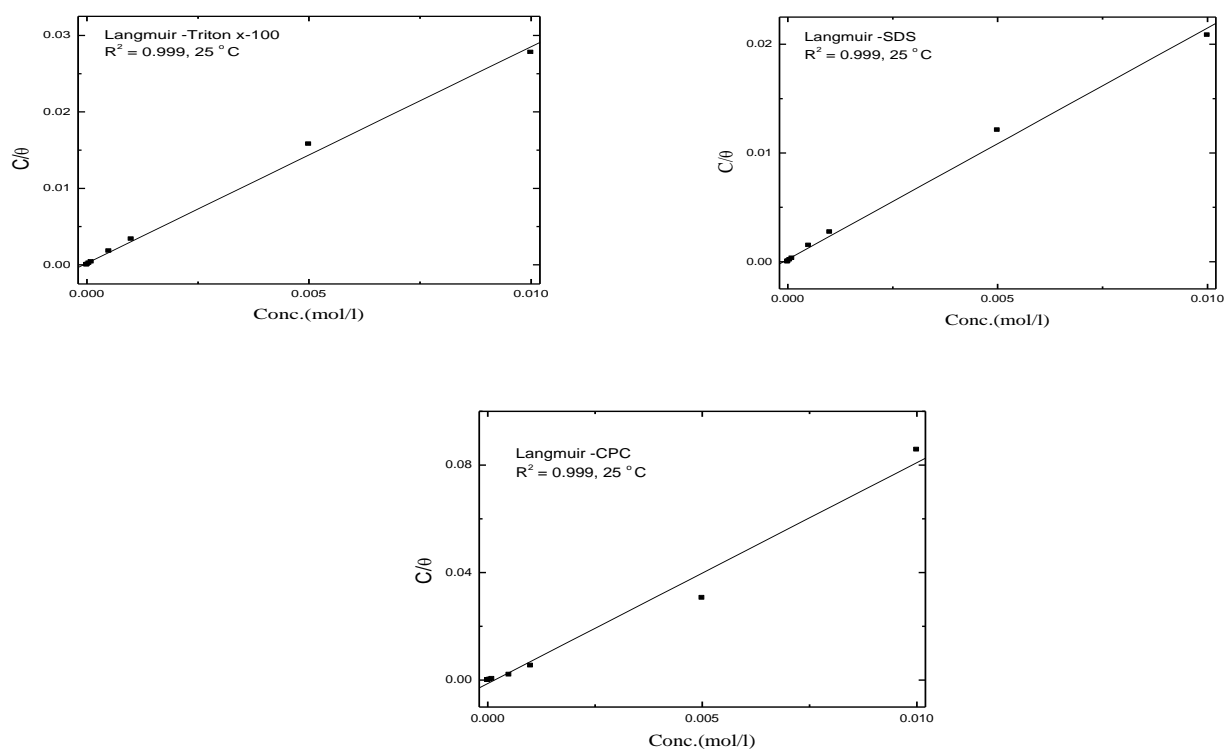
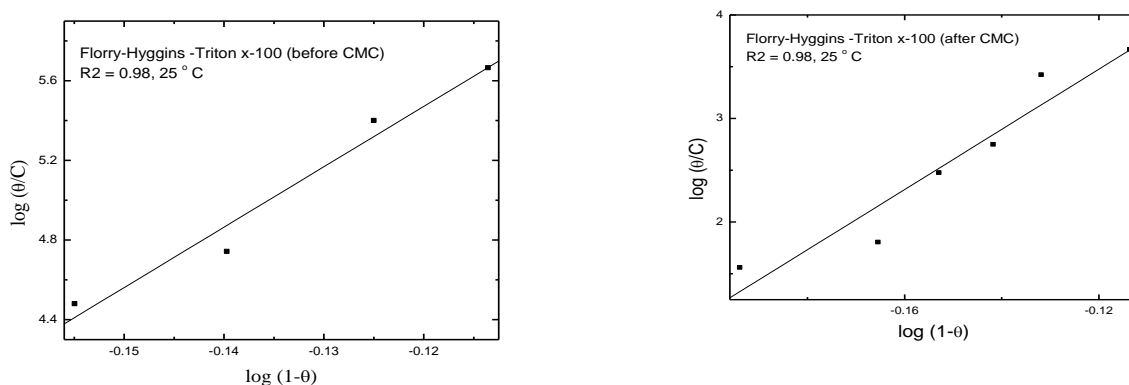


Fig 9 . Langmuir adsorption isotherm using impeller at 375 rpm for a) Triton x-100 b)SDS and c)CPC at 25° C



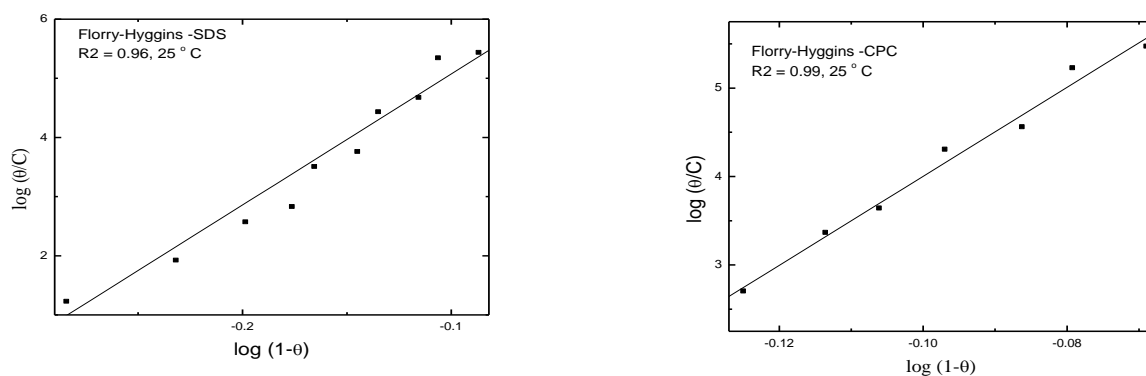


Fig 10 . Florry-Hyggins adsorption isotherm using impeller at 375 rpm for a) Triton x-100 (before CMC) , b) Triton x-100 (after CMC) c)SDS and d)CPC at 25° C

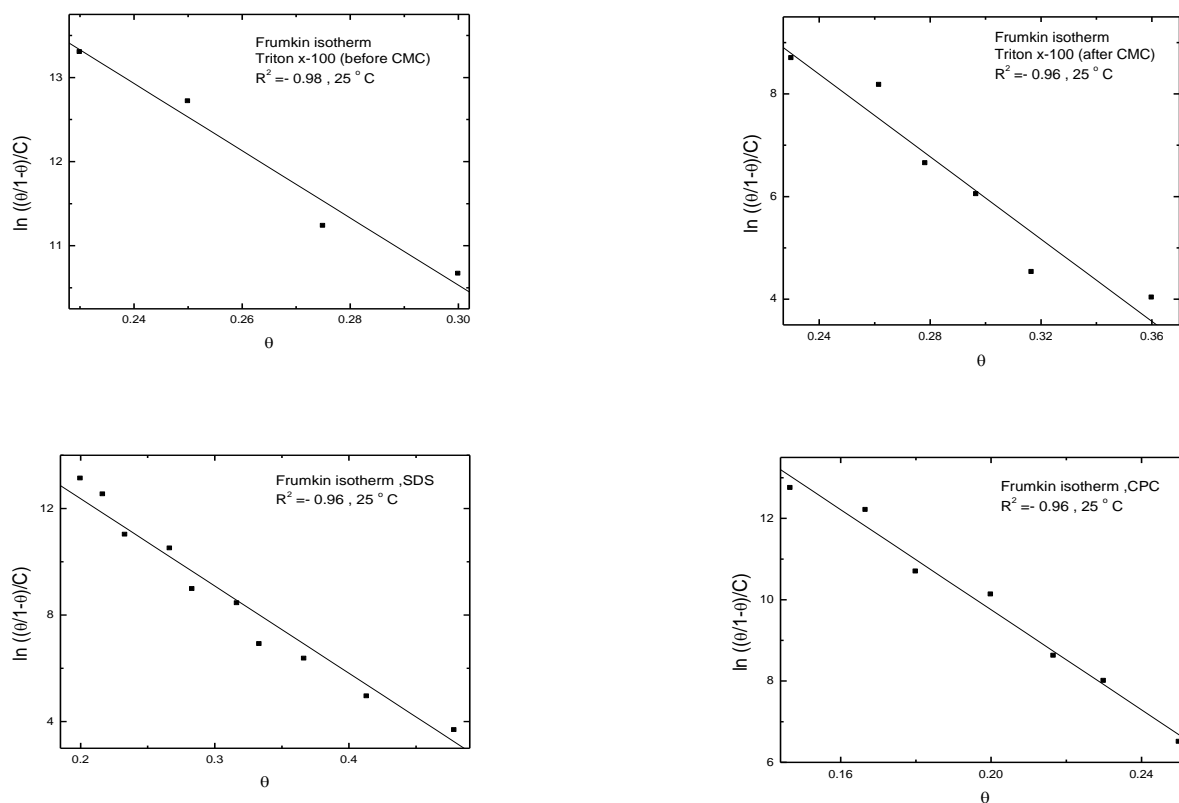


Fig 11 . Frumkin adsorption isotherm using impeller at 375 for a) Triton x-100 (before CMC) , b) Triton x-100 (after CMC) c)SDS and d)CPC at 25° C

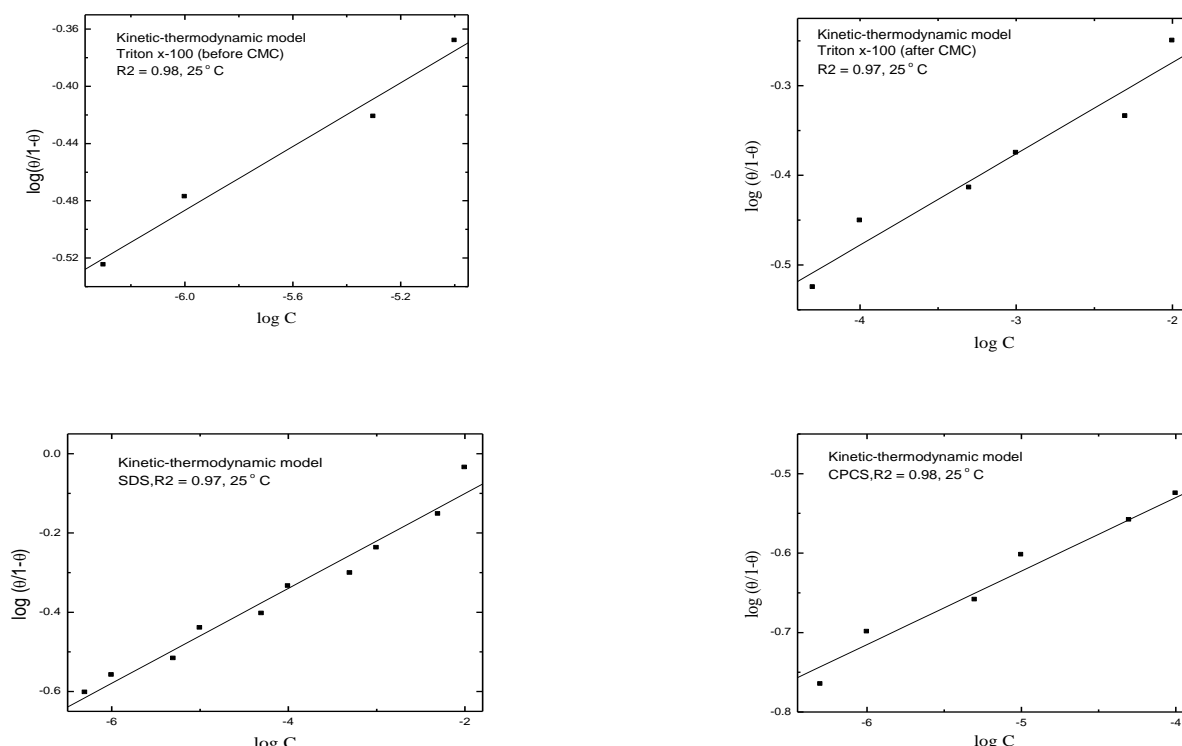


Fig 12 . Kinetic-thermodynamic adsorption isotherm using impeller at 375 rpm a) Triton x-100 (before CMC) , b) Triton x-100 (after CMC) c)SDS and d)CPC at 25°C

3.7. Data correlation

An overall mass transfer correlation was considered using the dimensionless groups Sh, Sc and Re which are often used to correlate mass transfer data in agitated system. Where Sh, Sherwood number ($Sh = K d_e/D$), K is mass transfer coefficient ($\text{cm} \cdot \text{sec}^{-1}$), d_e is the equivalent diameter of the vessel base area ($d_e = 4 \times \text{cross-sectional area} / \text{wetted perimeter}$, cm and D is diffusion coefficient $\text{cm}^2 \cdot \text{sec}^{-1}$), Sc, Schmidt number ($Sc = \nu/D$), ν is the kinematic viscosity, $\text{cm}^2 \cdot \text{sec}^{-1}$ and Re, Reynolds number ($Re = \rho N d^2 / \mu$), N is rotation per second of the impeller, rps, d is impeller diameter, cm, ρ is density of solution $\text{g} \cdot \text{cm}^{-3}$ and μ is solution viscosity ($\text{g} \cdot \text{cm}^{-1} \cdot \text{sec}^{-1}$)

The equivalent diameter of the vessel base area was used as a characteristic length in calculating Sh, while the impeller diameter was used as a characteristic length in calculating Re

Fig. 13 shows that the data for the four-blade turbine impeller under the condition

$$1045 < Sc < 3969$$

$$193 < Re < 1882$$

Fit the following equation

Received: 02 January 2025

Revised: 09 January 2025

Accepted: 17 January 2025

Copyright © authors 2025

DOI: <https://doi.org/10.5281/ZENODO.14680390>

Blank	$Sh = 6.98 Sc^{0.33} Re^{0.38} \pm 0.034$
Tritonx-100	$Sh = 7.24 Sc^{0.33} Re^{0.35} \pm 0.026$
SDS	$Sh = 9.12 Sc^{0.33} Re^{0.34} \pm 0.044$
CPC	$Sh = 9.12 Sc^{0.33} Re^{0.35} \pm 0.023$

Fluid dynamics studies of agitated vessels have shown that laminar flow prevails at $Re < 10$ while turbulent flow prevails at $Re > 10000$. in the transition zone , $10 < Re < 10000$, which dominate in the present study . the flow was turbulent at the impeller zone and laminar in remote parts of the vessel [24].

The lower value of exponent of Re number support the above assumption

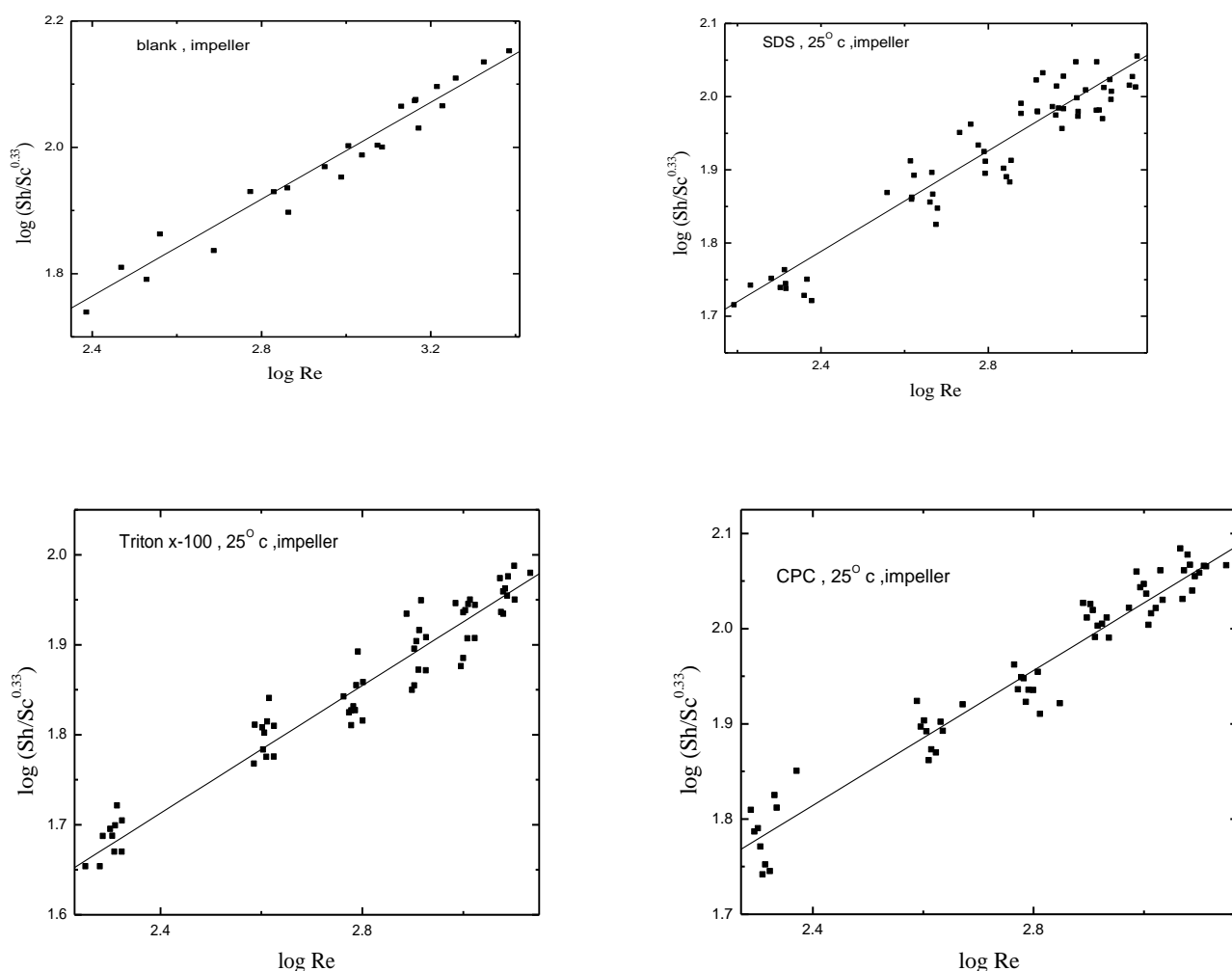


Fig. 13. The overall mass transfer correlation for the dissolution process in the absence and presence of different SAS at 25°C in an agitated vessel

3.8. Scanning electron microscope (SEM)

Fig.14a shows the SEM image for the copper surface before dissolution in which a rough, matt and uneven surface was seen also large deep cavities and small pits are distributed over the surface. Fig (14b-f) shows the surface morphology of copper that were dissolved at 25°C with different impeller rotations speeds 125, 250, 500, 750 and 1000 rpm in 8 M H_3PO_4 .

A bad and uneven surface appearance is obtained before electro-dissolution (Fig 14.a) where cavities and large deep pits are represented) [25,26].

We can say that, the radial flow for diffusion of the Cu^{2+} is disturbed at lower (125 , 250 rpm) (Fig b , c) and higher rotation speed 750 and 1000 rpm (Fig e , f) which leads to the dissimilar dissolution of copper .

The surface appearance is enhanced in moderate rotation speed, 500 rpm (Fig d) in which smooth and completely uniform surface is obtained.

This behavior is attributed to similar dissolution of copper and levelling effect .

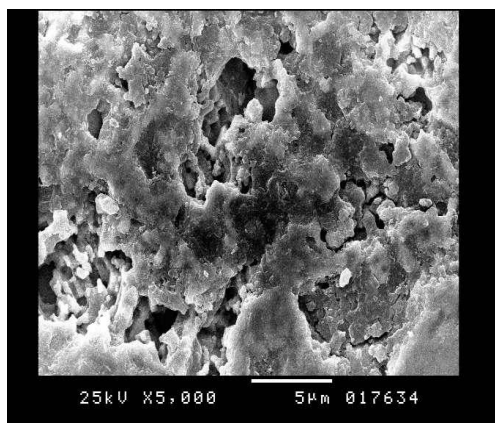


Fig14a. raw sample (before EP)

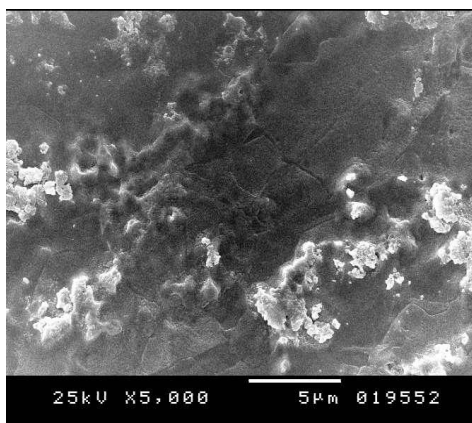


Fig.14b.after EP, 8 M H_3PO_4 ,125 rpm



Fig.14c.after EP, 8 M H_3PO_4 ,250 rpm

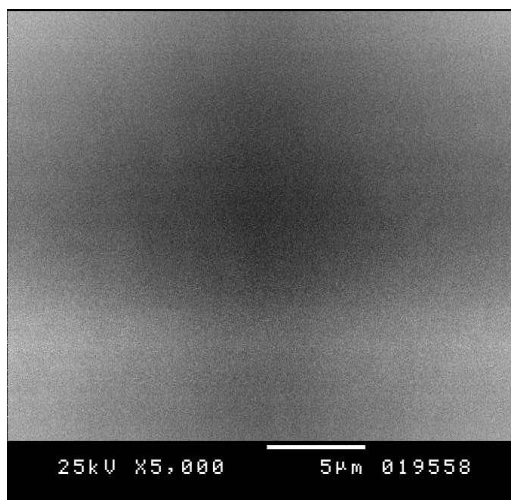


Fig.14d.after EP, 8 M H₃PO₄ ,500 rpm

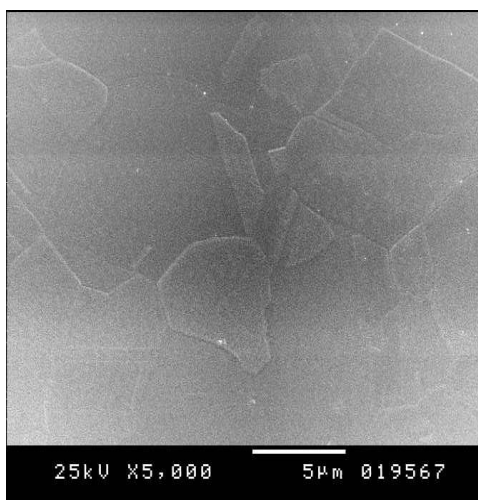


Fig.14e.after EP, 8 M H₃PO₄ ,750 rpm

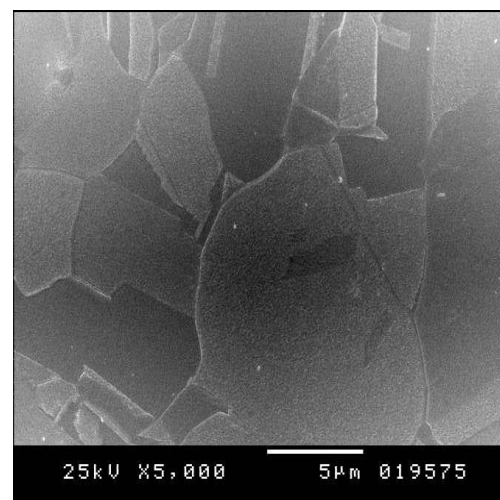


Fig.14f.after EP, 8 M H₃PO₄ ,1000 rpm

Figure 14. Surface morphologies of the copper at 25° C a) before-electro -dissolution b) after electro -dissolution in 8M H₃PO₄ 125 rpm , c) 250 rpm , d) 500 rpm, e) 750 rpm and f) at 1000 rpm

CONCLUSIONS

- As the impeller's rotation rate increases, the measured value of the dissolution process limiting current increases.
- With increasing the concentration of the used SAS, the limiting current decreases, and their inhibition efficiency decreases due to their tendency towards adsorption.
- Ea values of SAS were larger than that of 8MH₃PO₄ free solution, suggesting that the adsorption of SAS molecules leads to an increase in the energy barrier of copper dissolution.
- SAS's adsorption obeys a kinetic–thermodynamic isotherm, which indicates that the main process of inhibition is adsorption. Values of ΔG°_{ads} indicate that the adsorption process is physical adsorption.
- In the presence of the three studied surfactants, surface morphology enhanced for the copper surface at the moderate impeller rotation speed

References

- [1] Taha, A. A., Rahman, H. H. A., & Abouzeid, F. M. (2013). Effect of surfactants on the rate of diffusion controlled anodic dissolution of copper in orthophosphoric acid. *International Journal of Electrochemical Science*, 8(5), 6744-6762. [https://doi.org/10.1016/S1452-3981\(23\)14801-2](https://doi.org/10.1016/S1452-3981(23)14801-2)
- [2] Abouzeid . F.M and ALSHAMMERY.S(2021)., Physico-Chemical Studies of Almond Shell Extracts Potential on the Electropolishing and Electrorefining of Copper, *Asian.J.chem* 33(10). 2333-2340
<https://doi.org/10.14233/ajchem.2021.23298>
- [3] Taha, A. A., Rahman, H. H. A., Ahmed, A. M., & Abouzeid, F. M. (2013). A study of factors influencing on dissolution behavior of copper in orthophosphoric acid using rotating cylinder electrode (RCE) and rotating disc electrode (RDE). *International Journal of Electrochemical Science*, 8(7), 9041-9059. [https://doi.org/10.1016/S1452-3981\(23\)12948-8](https://doi.org/10.1016/S1452-3981(23)12948-8)
- [4] Abouzeid, F. M. (2016). Comparison between electropolishing behavior of copper and mild steel in the presence of lactic and mandolic acid. *International Journal of Electrochemical Science*, 11(8), 7269-7281. <https://doi.org/10.20964/2016.08.20>
- [5] Taha, A. A., Abouzeid, F. M., Elsadek, M. M., & Habib, F. M. (2020). Effect of methanolic plant extract on copper electro-polishing in ortho-phosphoric acid. *Arabian Journal of Chemistry*, 13(8), 6606-6625. <https://doi.org/10.1016/j.arabjc.2020.06.017>
- [6] Abouzeid, F. M., & Alshammery, S. (2022). The hibiscus extract potential in inhibiting anodic dissolution of copper. *Revista De Chimie (Bucuresti)*, 73(3), 67-81. <https://doi.org/10.37358/RC.22.3.8536>
- [7] yamsuir, S., Susetyo, F. B., Anggrainy, R., Lubi, A., Soegijono, B., Rosyidan, C., Yudanto, S. D., Situmorang, E. U. M., & Nanto, D. (2024). Electrolyte solution stirring effect on deposition rate, crystallographic orientation, and electrochemical behaviour of ni film. *Journal of Physics. Conference Series*, 2866(1), 12001. <https://doi.org/10.1088/1742-6596/2866/1/01200>
- [8] Vinod Kumaar, J. R., Thanigaivelan, R., & Soundarrajan, M. (2022). A performance study of electrochemical micro-machining on SS 316L using suspended copper metal powder along with stirring effect. *Materials and Manufacturing Processes*, 37(13), 1526-1539. <https://doi.org/10.1080/10426914.2022.2030874>
- [9] Samuel, J. O. E., Rathinavel, N., Veleeswaran, A., Thulasinathan, B., Ramalingam, K. R., Rathinam, Y., & Alagarsamy, A. (2024). New insight on the influence of surface-modified clay cup with stirring effect for bioelectricity production by utilizing septic tank wastewater. *Process Safety and Environmental Protection*, 186, 213-223. <https://doi.org/10.1016/j.psep.2024.03.110>
- [10] Taha, A. A., Rahman, H. H. A., & Abouzeid, F. M. (2013). Effect of surfactants on the rate of diffusion controlled anodic dissolution of copper in orthophosphoric acid. *International Journal of Electrochemical Science*, 8(5), 6744-

6762. [https://doi.org/10.1016/S1452-3981\(23\)14801-2](https://doi.org/10.1016/S1452-3981(23)14801-2)

- [11] Fořt, I., Seichter, P., & Peřl, L. (2013). Axial thrust of axial flow impellers. *Chemical Engineering Research & Design*, 91(5), 789-794. <https://doi.org/10.1016/j.cherd.2012.10.001>
- [12] Taha, A. A., Abouzeid, F. M., & Kandil, M. M. (2020). Some drugs effect on the electropolishing of C-steel in H3PO4 acid under normal and compulsory convection circumstances. *Russian Journal of Electrochemistry*, 56(3), 189-205. <https://doi.org/10.1134/S102319352003012X>
- [13] Fatma, M. A. (2015). A study of the morphology and optical properties of electro polished steel in the presence of vitamin-C. *African Journal of Pure and Applied Chemistry*, 9(6), 135-145. <https://doi.org/10.5897/AJPAC2015.0631>
- [14] El-Sayed, A. A. M., Abouzeid, F. M., Ismail, M. M., & ElZokm, G. M. (2021). Characterization and utilization of sargassum linifolium and stypopodium schimperi polysaccharides as blue inhibitors for steel electro-polishing. *Water Science and Technology*, 83(2), 409-424. <https://doi.org/10.2166/wst.2020.586>
- [15] Seyam, D. F., H. Tantawy, A., Eid, S., & El-Etre, A. Y. (2022). Study of the inhibition effect of two novel synthesized amido-amine-based cationic surfactants on aluminum corrosion in 0.5 M HCl solution. *Journal of Surfactants and Detergents*, 25(1), 133-143. <https://doi.org/10.1002/jsde.12546>
- [16] Elaraby, A., El-samad, S. A., khamis, E. A., & Zaki, E. G. (2023). Theoretical and electrochemical evaluation of tetra-cationic surfactant as corrosion inhibitor for carbon steel in 1 M HCl. *Scientific Reports*, 13(1), 942-942. <https://doi.org/10.1038/s41598-023-27513-7>
- [17] Attia, A., & Abdel-Fatah, H. T. M. (2020). Triton X-100 as a non-ionic surfactant for corrosion inhibition of mild steel during acid cleaning. *Metals and Materials International*, 26(11), 1715-1724. <https://doi.org/10.1007/s12540-019-00533-7>
- [18] Yaagoob, I. Y., Goni, Lipiar K. M. O., Verma, C., Mazumder, M. A. J., & Ali, S. A. (2023). N-(4-Chloromethylbenzyl)-N, N-dimethyldodecan-1-aminium chloride: A quaternary ammonium surfactant as corrosion inhibitor. *ChemistrySelect* (Weinheim), 8(38)<https://doi.org/10.1002/slct.202301913>
- [19] Frank, F., Tomasetig, D., Nahrngbauer, P., Ipsmiller, W., Mauschitz, G., Wieland, K., & Lendl, B. (2024). study of the interactions between metal surfaces and cationic surfactant corrosion inhibitors by surface-enhanced raman spectroscopy coupled with visible spectroscopy. *Analyst (London)*, 149(22), 5372-538. <https://doi.org/10.1039/d4an00861h>
- [20] Wu, C., Yang, H., Zhang, S., Han, P., Sun, H., Sheng, Z., Yu, H., & Ma, X.

- (2023). The inhibition performance of anionic surfactant and zwitterionic surfactant toward the corrosion of carbon steel in NaCl solution. *International Journal of Chemical Kinetics*, 55(9), 537-550. <https://doi.org/10.1002/kin.21654>
- [21] Zhuang, W., Wang, X., Zhu, W., Zhang, Y., Sun, D., Zhang, R., & Wu, C. (2021). Imidazoline gemini surfactants as corrosion inhibitors for carbon steel X70 in NaCl solution. *ACS Omega*, 6(8), 5653-5660. <https://doi.org/10.1021/acsomega.0c06103>
- [22] Abouzeid, F. M. A., & Alshammery, S. (2024). ,Effect of Green Additives in Copper Electrefining Bath: Current Efficiency and Surface Characterization Investigation, *journal of chemistry* 1-24. <https://doi.org/10.1155/joch/5758810>
- [23] Čelan, A., Ćosić, M., Pehneć, I., & Kuzmanić, N. (2019). Influence of impeller diameter on crystal growth kinetics of borax in a mixed Dual-Impeller Batch-Cooling crystallizer. *Chemical Engineering & Technology*, 42(4), 788-796. <https://doi.org/10.1002/ceat.201800609>
- [24] Wu, M., Jurtz, N., Hohl, L., & Kraume, M. (2024). Multi-impeller mixing performance prediction in stirred tanks using mean age theory approach. *AIChE Journal*, 70(1), n/a. <https://doi.org/10.1002/aic.18247>
- [25] Abouzeid, F. M., & Abubshait, H. A. (2020). A study of vitamin B influence on the morphology, roughness, and reflectance of electropolished aluminum in H3PO4–H2SO4 mixture. *Arabian Journal of Chemistry*, 13(1), 2579-2595. <https://doi.org/10.1016/j.arabjc.2018.06.011>
- [26] Abouzeid, F. M. A., & Alshammery, S. (2024). Characterization and utilization of apple peel and grape stems extract constituents as green restraints for aluminum dissolution. *Scientific Reports*, 14(1), 24170-18. <https://doi.org/10.1038/s41598-024-73592-5>